4. Martino E, Murtas ML, Loviselli A, et al. Percutaneous intranodular ethanol injection for treatment of autonomously functioning thyroid nodules. *Surgery* 1992;112:1161–1165.
5. Papini E, Panunzi C, Pacella CM, et al. Percutaneous ultrasound-guided ethanol injection: a new treatment of toxic autonomously functioning thyroid nodules? *J Clin Endocrinol Metab* 1993;76:411–416.
6. Mazzeo S, Toni MG, De Gaudio C, et al. Percutaneous injection of ethanol to treat autonomous thyroid nodules. *Am J Roentgenol* 1993;161:871–876.
7. Livraghi T, Paracchi A, Ferrari C, Reschini E, Macchi RM, Bonifacino A. Treatment of autonomous thyroid nodules by percutaneous ethanol injection: a 4-year experience. *Radiology* 1994;190:529–533.
8. Ozdemir H, Ilgit ET, Yucel C, et al. Treatment of autonomous thyroid nodules: safety and efficacy of sonographically guided percutaneous injection of ethanol. *Am J Roentgenol* 1994;163:929–932.
9. Braun B, Blank W. Farbdopplersonographisch gestenerte perkutane alkoholinstillation zur therapie der funktionellen schilddrusenautonomie. *Dtsch Med Wochenschr* 1994; 119:1607–1612.
10. Di Lelio A, Rivolta MR, Casati M, Capra M. Treatment of autonomous thyroid nodules: value of percutaneous ethanol injection. *Am J Roentgenol* 1995;164:207–213.
11. Hay ID, Morris JC. Toxic adenoma and toxic multinodular goiter. In: Braverman LE, Utiger RD, eds. *Werner and Ingbar's the thyroid: A fundamental and clinical text*, 7th ed. Philadelphia-New York: Lippincott-Raven; 1996:566–572.
12. Reschini E, Catania A, Ferrari C, Bergonzi M, Paracchi A, Raineri P. Comparison of pertechnetate and radioiodine thyroid scintiscans in thyroid disease. *J Nucl Biol Med* 1993;37:12–17.
13. Reschini E, Matheoud R, Canzi C, et al. Absorbed dose estimate in nodular and extranodular tissue by quantitative iodine-123 imaging before iodine-131 radiotherapy for autonomous thyroid adenoma [Abstract]. *J Nucl Med* 1996;37(suppl):230P.
14. Berman M, Braverman LE, Burke J, et al. Report No. 5. I-123, I-124, I-125, I-126, I-130, I-131, and I-132 as sodium iodide. In: Loevinger R, Budinger TF, Watson EE, eds. *MIRD primer for absorbed dose calculations*. New York: Society of Nuclear Medicine; 1988:49–54.
15. Solomon DH. Factors affecting the fractional rate of release of radioiodine from the thyroid gland in man. *Metabolism* 1956;5:667–681.
16. Romelli PB, Pennisi F, Vancheri L. Measurement of free thyroid hormones in serum by adsorption chromatography and radioimmunoassay. *J Endocrinol Invest* 1979;2: 25–40.
17. Molnar GD, Wilber RD, Lee RE, Woolner LB, Keating FR. On the hyperfunctioning solitary thyroid nodule. *Mayo Clin Proc* 1965;40:665–684.
18. Horst W, Rosler H, Schneider C, Labhart A. Three-hundred six cases of toxic adenoma: clinical aspects, findings in radioiodine diagnostics, radiochromatography and histology; results of ^{131}I and surgical treatment. *J Nucl Med* 1967;8:515–528.
19. Blum M, Shenkman L, Hollander CS. The autonomous nodule of the thyroid: correlation of patient age, nodule size and functional status. *Am J Med Sci* 1975;269: 43–50.
20. Ng Tang Fui SC, Maisey MN. Standard dose ^{131}I therapy for hyperthyroidism caused by autonomously functioning thyroid nodules. *Clin Endocrinol (Oxford)* 1979;10:69–77.
21. Kinser JA, Roesler H, Furrer T, Grutter D, Zimmermann H. Nonimmunogenic hyperthyroidism: cumulative hypothyroidism incidence after radioiodine and surgical treatment. *J Nucl Med* 1989;30:1960–1965.
22. Nygaard B, Jarlov AE, Hegedus L, Schaadt B, Kristensen LO, Hansen JM. Long-term follow-up of thyroid scintigraphies after ^{131}I therapy of solitary autonomous thyroid nodules. *Thyroid* 1994;4:167–171.
23. Ferrari C, Reschini E, Paracchi A. Treatment of the autonomous thyroid nodule: a review. *Eur J Endocrinol* 1996;135:383–390.
24. Clerc J, Dagousset F, Izembart M, et al. Radioiodine therapy of the autonomous thyroid nodule in patients with or without visible extranodular activity. *J Nucl Med* 1995;36:217–223.

Fluorine-18-FDG PET Imaging Is Negative in Bronchioloalveolar Lung Carcinoma

Kotaro Higashi, Yoshimichi Ueda, Hiroyasu Seki, Kokichi Yuasa, Manabu Oguchi, Tetsuhiko Noguchi, Mitsuru Taniguchi, Hisao Tonami, Tetsuro Okimura and Itaru Yamamoto

Departments of Radiology, Internal Medicine, Pathology and Thoracic Surgery, Kanazawa Medical University, Kahoku-gun, Ishikawa; and Department of Radiology, Kanazawa Cardiovascular Hospital, Kahoku-gun, Ishikawa, Japan

The goals of our study were to establish PET accuracy with ^{18}F-fluorodeoxyglucose (FDG) in finding localized formations of bronchioloalveolar lung carcinoma (BAC) and to investigate the correlation between FDG uptake and the degree of cell differentiation in adenocarcinoma of the lung. **Materials:** Twenty-nine patients with 30 adenocarcinomas of the lung (7 bronchioloalveolar lung carcinomas, 9 well differentiated, 2 well-moderately differentiated, 11 moderately differentiated and 1 poorly differentiated) were studied. All patients underwent thoracotomies within 4 wk after the FDG PET study. For qualitative analysis, the degree of FDG activity in the tumors was visually scored using a five-point grading system: 0 = same to background activity, 1 = less than mediastinal blood-pool activity, 2 = same to mediastinal blood-pool activity, 3 = slightly greater than mediastinal blood-pool activity and 4 = substantially greater than mediastinal blood-pool activity. Foci of activity with Grades 2–4 were considered tumors. For semiquantitative analysis, standardized uptake values (SUV) were calculated. **Results:** In 7 BACs, 4 lesions (57%) showed negative results on FDG PET, while in 23 non-BACs, only 1 lesion (4%), which was a well-differentiated adenocarcinoma showed a negative result. BACs' mean visual score (1.43 ± 1.27) was significantly lower than that of non-BACs (3.17 ± 1.03) ($p = 0.001$). The BACs' mean SUV (1.36 ± 0.821) was significantly lower than that of well-differentiated adenocarcinomas (2.92 ± 1.28) ($p = 0.014$); the mean SUV of well-differentiated adenocarcinomas was significantly lower than that of moderately differentiated adenocarcinomas (4.63 ± 1.86) ($p = 0.031$). No significant differences were apparent in average size among these three histologic types. **Conclusion:** A correlation was observed between FDG uptake and the degree of cell differentiation in adenocarcinoma of the lung. FDG PET may show negative results for BAC.

Key Words: PET; fluorine-18-fluorodeoxyglucose; bronchioloalveolar lung carcinoma

J Nucl Med 1998; 39:1016–1020

PET with ^{18}F-fluorodeoxyglucose (FDG) may play a valuable role in delineating viable tumor tissue due to FDG PET's ability to detect a tumor's increased glucose metabolism. It is known that malignant tumors tend to show higher metabolic demands than normal tissues. Recent articles have indicated FDG PET's value in diagnosing human lung cancer (*1–7*). FDG PET has a sensitivity and specificity of 93% and 88%, respectively, for detecting malignancy in indeterminate solitary pulmonary nodules (*7*). However, wide variations in glucose consumption exist among individuals depending on the type of neoplasm. In cases of malignant lung neoplasms, few negative results of malignancy have been reported using FDG PET (*4,5,8*). Negative results have occurred in patients with bronchioloalveolar lung carcinomas (BACs) (*4,8*). BAC is a form of peripheral lung adenocarcinoma growing as a single layer of malignant cells along the walls of terminal airways (*9*). It is known that the tumor growth rate for BACs is lower than that for non-BAC

Received May 2, 1997; accepted Sep. 4, 1997.

For correspondence or reprints contact: Kotaro Higashi, MD, Department of Radiology, Kanazawa Medical University, 1–1, Daigaku, Uchinada, Kahoku-gun, Ishikawa, 920–02, Japan.

adenocarcinomas (*10*). In certain tumor cell types, glucose metabolism measured by FDG PET varies proportionately with the cells proliferative activity and malignancy grade (*11–17*). There are few reports of FDG PET revealing a localized BAC formation or of a correlation between FDG uptake and the degree of cell differentiation in lung cancers. We designed our study to assess FDG PET's ability to find localized BAC formations and to assess the correlation between FDG uptake and the degree of cell differentiation in adenocarcinoma of the lung.

MATERIALS AND METHODS

Patients

Twenty-nine patients (12 men, 17 women; age range 46–81 yr; mean age 63 yr) with 30 adenocarcinomas of the lung who had undergone both preoperative FDG PET imaging and thoracotomies during February 1994 and November 1996 were enrolled in our study. One patient had 2 adenocarcinomas. All patients underwent thoracotomies within 4 wk after FDG PET study. In all patients, final diagnoses were established by histologies (thoracotomies). The sizes of the primary tumors were determined from the resected specimens and ranged from 1–4.9 cm. Twelve (40%) of the lung tumors were 2 cm or less than 2 cm in diameter. Of the remaining 18 tumors, 9 were 2.1 cm to 3 cm, and 9 were greater than 3 cm in size. None of the patients had insulin-dependent diabetes, and the serum glucose levels in all patients just before the FDG was injected were less than 120 mg/dl. Informed consent was obtained from each patient who participated in our study.

The surgically-resected tumors were fixed routinely in formalin and embedded in paraffin. All of the 5-mm sections, including the largest cut tumor surfaces, were stained with hematoxylin and eosin and examined by light microscopy. Adenocarcinomas of the lung were subgrouped into BACs and non-BACs. Non-BACs were subgrouped into well, moderately and poorly differentiated adenocarcinomas according to the World Health Organization classification of lung tumors (*18*). Of 30 adenocarcinomas, 7 were BACs and 23 were non-BACs. Of 23 non-BACs, 9 were categorized as well differentiated, 2 as well-moderately differentiated, 11 as moderately differentiated and 1 as poorly differentiated.

Preparation of Fluorine-18-FDG

Fluorine-18 was produced by ^{20}Ne (d, α) ^{18}F nuclear reaction, and FDG was synthesized by the acetyl hydrofluorite method.

FDG PET

PET was performed using a PET camera (Headtome IV, Shimazu, Kyoto, Japan) having four rings, which provided 7 tomographic slices. Its intrinsic resolution was 5-mm FWHM at the center. After at least 4 hr of fasting, each subject underwent 10 min of transmission scanning for attenuation correction using a ^{68}Ge ring source. Immediately after the transmission scan, FDG was administered intravenously. Forty minutes later, static scans of 10–20 min (14–24 tomographic slices at 6.5-mm intervals) were performed using a 128 × 128 matrix. The average injection dose of FDG was 148 MBq (4 mCi) and ranged from 104 MBq (2.8 mCi) to 318 MBq (8.6 mCi). The average injection dose of FDG in our study was approximately one-half dose, which was reported previously (*2,3*). The effects of variance on the injection doses has been evaluated previously (*26*), therefore, no significant correlation was observed between the injection dose and the tumor-to-muscle radioactivity ratio, although the image quality and s.d. of the region of interest (ROI) data had deteriorated in the small injection dose. In our study, the patients' body weights ranged from 39.2 kg to 75.0 kg with a mean of 52.5 kg. The FDG injection dose was reduced in cases of low body weight.

Data Analysis

Two readers visually interpreted the FDG images on the films and correlated them with contemporaneous CT studies. For qualitative analysis, the degree of FDG activity in the tumors was visually scored using a five-point grading system: 0 = same to background activity, 1 = less than mediastinal blood-pool activity, 2 = same to mediastinal blood-pool activity, 3 = slightly greater than mediastinal blood-pool activity, and 4 = substantially greater than mediastinal blood-pool activity. For qualitative analysis, foci of activity with Grades 2–4 were considered positive for tumors. For semiquantitative analysis of the FDG uptake, ROIs were placed over the most intense area of FDG accumulation. In some patients, no nodules could be detected on the PET. In these patients, the ROI was drawn in its location as extrapolated from chest CT scans. After correction for radioactive decay, we analyzed the ROIs by computing the standardized uptake value (SUV). SUV was computed as follows:

$$\text{Mean PET counts/pixel/sec} \times \text{calibration factor/injected dose}$$

$$(\mu\text{Ci})/\text{body weight (Kg)}, \text{ where calibration factor}$$

$$= (\mu\text{Ci/ml})/(\text{counts/pixel/sec}).$$

No recovery coefficient correction was applied.

Statistical Analysis

Comparison of the differences in FDG uptake was performed using the two-tailed Student's t-test for unpaired data. Probability values of < 0.05 were considered statistically significant.

RESULTS

Table 1 summarizes the results of the radionuclide and pathologic findings for the 29 patients (30 adenocarcinomas) in the study. In 7 BACs, FDG PET showed negative results on 4 lesions (Grade 0 = 2 lesions; Grade 1 = 2 lesions). A typical example (Patient 1) is presented in Figure 1. Of the remaining 3 BACs, 1 was Grade 2 and 2 were Grade 3. No cases of BACs showed Grade 4. In 23 non-BACs, only 1 lesion (4%), which was a well-differentiated adenocarcinoma (Patient 8) showed a negative result. Of the remaining 22 non-BACs, 7 were Grade 2, 2 were Grade 3 and 13 were Grade 4. The BACs' mean visual score (1.43 ± 1.27) was significantly lower than that of the non-BACs (3.17 ± 1.03) ($p = 0.001$) (Fig. 2), while no significant difference in average size was observable between BACs (2.57 ± 1.03 cm) and non-BACs (2.61 ± 1.02 cm). The BACs' mean SUV (1.36 ± 0.821) was significantly lower than that of well-differentiated adenocarcinomas (2.92 ± 1.28) ($p = 0.014$) (Fig. 3), and the mean SUV of well-differentiated adenocarcinomas was significantly lower than that of moderately differentiated adenocarcinomas (4.63 ± 1.86) ($p = 0.031$) (Fig. 3). These three histological types showed no significant differences in average size (BACs 2.57 ± 1.03 cm, well-differentiated adenocarcinoma 2.52 ± 0.91 cm, and moderately differentiated adenocarcinoma 2.91 ± 1.1 cm, respectively). An example of a well-differentiated adenocarcinoma (Patient 11) is in Figure 4, and its SUV (1.24) was relatively low. A case of a poorly differentiated adenocarcinoma was included in our study (Patient 30, Fig. 5), and its SUV (6.13) was relatively high. Thus, a correlation was seen between FDG uptake and degree of cell differentiation in adenocarcinoma of the lung.

DISCUSSION

BAC is a form of lung cancer exhibiting many features that distinguish it from all other forms of lung cancer including non-BAC adenocarcinoma. Recent evidence suggests that the number of cases of adenocarcinoma of the lung has increased

TABLE 1
Patient Characteristics and FDG PET Imaging Results

Patient no.	Age (yr)	Sex	Histological type	Size (cm)	FDG score	FDG SUV
1	51	F	Bronchioalveolar ca.	1.2 × 1.0	0	0.38
2	54	F	Bronchioalveolar ca.	2.2 × 1.7	0	0.84
3	49	F	Bronchioalveolar ca.	2.5 × 2.5	1	1.03
4	49	F	Bronchioalveolar ca.	2.6 × 1.7	1	1.10
5*	74	F	Bronchioalveolar ca.	1.7 × 0.9	2	1.27
6	68	F	Bronchioalveolar ca.	3.8 × 3.7	3	2.78
7	67	M	Bronchioalveolar ca.	4.0 × 3.7	3	2.14
8	58	M	Well diff. adenoca.	2.4 × 2.0	1	1.70
9	51	M	Well diff. adenoca.	1.7 × 1.5	2	2.03
10	46	M	Well diff. adenoca.	1.9 × 1.5	2	2.32
11	62	F	Well diff. adenoca.	2.0 × 2.0	2	1.24
12	50	F	Well diff. adenoca.	2.2 × 1.6	2	2.34
13	81	F	Well diff. adenoca.	1.8 × 1.6	4	4.52
14	64	F	Well diff. adenoca.	3.0 × 2.2	4	3.25
15	70	M	Well diff. adenoca.	3.2 × 2.6	4	4.41
16	79	F	Well diff. adenoca.	4.5 × 4.0	4	4.48
17	65	F	Well-mod. diff. adenoca.	1.0 × 1.0	2	2.41
18	75	M	Well-mod. diff. adenoca.	1.8 × 1.3	4	2.52
19	47	F	Mod. diff. adenoca.	1.6 × 1.0	2	2.04
20	59	F	Mod. diff. adenoca.	3.5 × 2.2	2	2.12
21	70	F	Mod. diff. adenoca.	1.5 × 1.5	3	2.64
22	73	F	Mod. diff. adenoca.	3.0 × 3.0	3	6.94
23	63	M	Mod. diff. adenoca.	1.8 × 1.2	4	3.81
24	60	F	Mod. diff. adenoca.	3.5 × 2.5	4	7.06
25	53	M	Mod. diff. adenoca.	2.9 × 2.9	4	5.76
26	68	M	Mod. diff. adenoca.	3.8 × 3.6	4	4.87
27	75	M	Mod. diff. adenoca.	4.9 × 3.2	4	6.05
28*	74	F	Mod. diff. adenoca.	1.9 × 1.8	4	3.76
29	64	M	Mod. diff. adenoca.	3.6 × 2.5	4	5.94
30	71	M	Poorly diff. adenoca.	2.5 × 2.0	4	6.13

*Same patient.

SUV = standardized uptake value; Well diff. = well differentiated; Well-mod. diff. = well-moderately differentiated; Mod. diff. = moderately differentiated; Poorly diff. = poorly differentiated; Adenoca = adenocarcinoma.

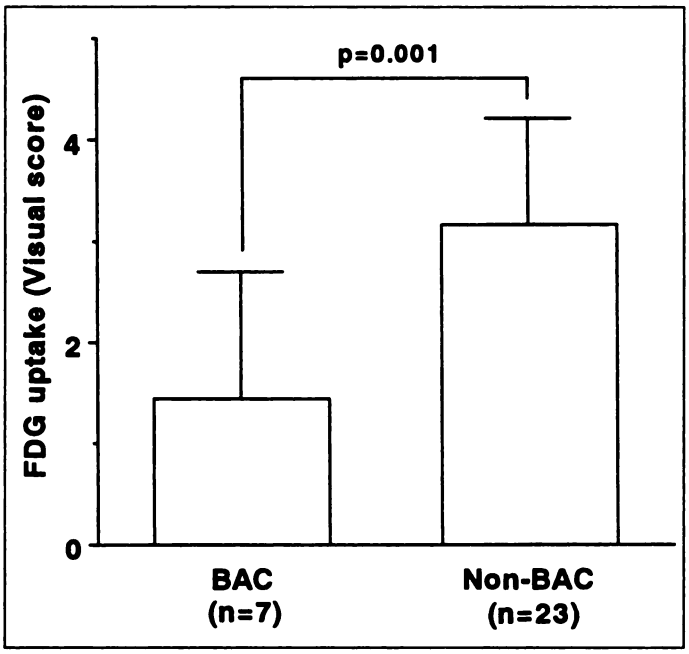

FIGURE 2. The mean visual score of BACs was significantly lower than that of non-BACs.

dramatically in the last decade and that this overall increase is largely due to an increase in BAC (*19,20*). It is known that the mean doubling time for BAC (300.1 days) is longer than that for non-BAC (224.6 days) (*10*). The proliferative potential for BAC is lower than that for well-differentiated adenocarcinomas (*21*). BAC also differs from non-BAC in that metastases are more frequent (*10*). Noguchi et al. (*22*) reported that localized BAC without foci of active fibroblastic proliferation showed no lymph node metastases and promises the most favorable prognosis of adenocarcinomas 2 cm or less in size. In BAC, p53 overexpression was particularly rare (*23*), and the activation of the ras oncogene was an infrequent event (*27*).

FDG PET is highly accurate in differentiating malignant from benign solitary pulmonary nodules (*7*). In our study, however, FDG PET showed negative results on 4 of 7 BACs, and we saw a significant correlation between FDG uptake and the degree of cell differentiation in adenocarcinoma of the lung. In cases of malignant lung neoplasms, few negative results for malignancy have been reported using FDG PET. A patient with BAC showed a negative PET result in a study conducted by Scott et al. (*4*). Jang et al. (*8*) also reported that FDG PET showed negative results for two BACs. These studies ascribed the negative results to low metabolic demands with a low-grade malignant potential of BAC. Negative results also occurred in patients with very small (<1 cm^2) lung cancers (*4*). A patient with a 1-cm nodule identified as a scar adenocarcinoma also showed a negative PET scan in a study by Dewan et al. (*5*). This study attributed the negative finding to the presence of relatively few malignant cells interspersed in a large amount of fibrous stroma, and the authors suggested that a critical mass of metabolically active malignant cells might be necessary to detect FDG uptake. In an in vitro study, FDG uptake was related to the number of viable cancer cells (*24*). In our study,

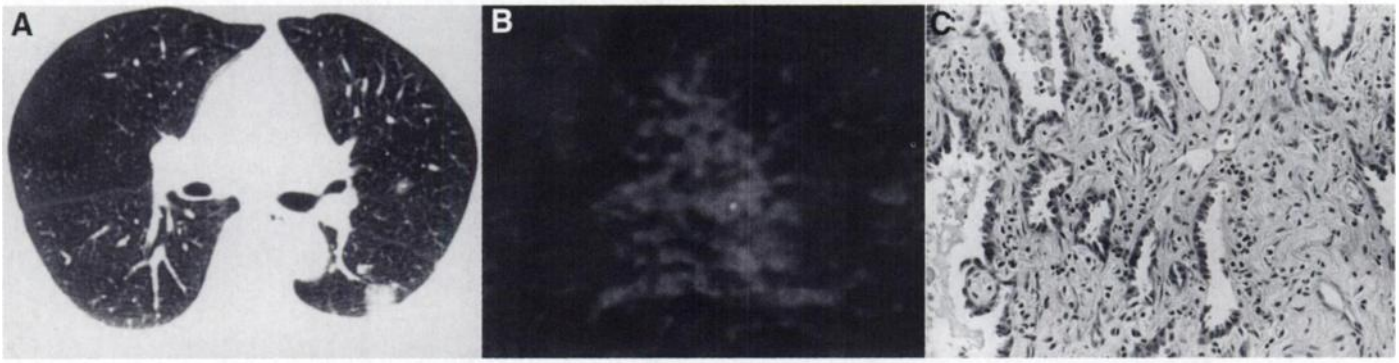

FIGURE 1. Patient 1: Bronchioloalveolar carcinoma, 1.2 × 1.0 cm, pT1N0M0. (A) CT image shows a nodule with ground-glass attenuation in the left lung posteriorly. Focal area of ground-glass attenuation at CT could be an early sign of localized bronchioloalveolar carcinoma (*8*). (B) FDG PET shows no significant accumulation in the tumor (FDG score 0, SUV 0.38). (C) High-power view shows a feature of a sclerosing variant of bronchioloalveolar carcinoma (hematoxyline and eosin stain; original magnification = × 225).

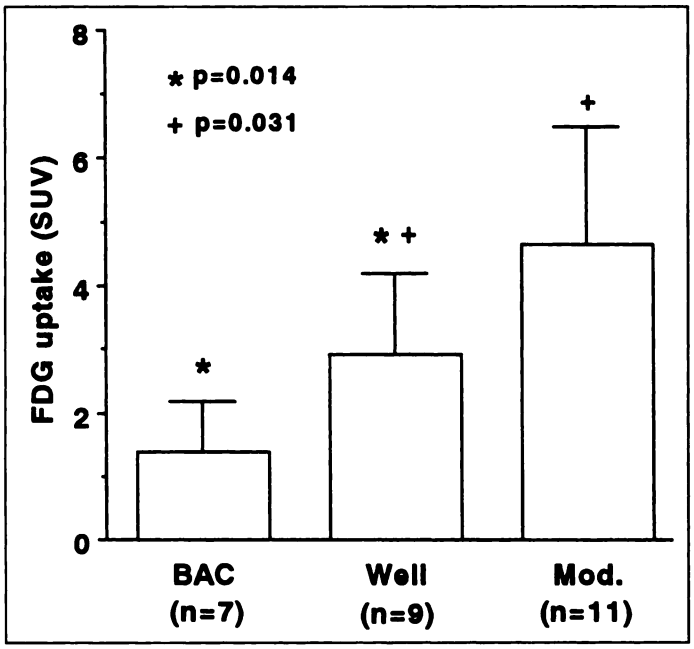

FIGURE 3. The mean SUV of BACs (BAC) was significantly lower than that of well-differentiated adenocarcinomas (Well), and the mean SUV of well-differentiated adenocarcinomas was significantly lower than that of moderately differentiated adenocarcinomas (Mod.).

a lesion as small as 1.0 cm demonstrated an increased FDG uptake. Additional factors that may hamper the detection of very small lesions include partial volume effects and respiratory motion. SUV is also affected by partial volume effects (*25*). In our study, however, we saw no significant difference in the average sizes of BACs and non-BACs.

We believe several reasons may account for our FDG PET tests producing negative results. It might be due partly to a low metabolic demand for glucose by generally slow-growing BAC or to the presence of a relatively small number of metabolically active malignant cells in BAC that appear as a focal area of ground-glass attenuation on CT. Several studies have confirmed the relationship between glucose metabolism measured by FDG PET and the growth rate or malignancy grade in different tumor types (*11–17*). In a study of 23 patients with primary cerebral tumors, Di Chiro et al. (*11*) established a link between the glycolytic activity measured by FDG PET and the rate of tumor growth in vivo. They postulated that a progressive increase in glucose metabolism accompanied the transformation from slow to rapid growing tumor. In a study of 13 patients with malignant head and neck tumors, Minn et al. (*12*) examined the relationship between glucose metabolism measured by FDG PET and tumor proliferative activity assessed by DNA flow cytometry. Their findings suggested that glucose metabolism correlated directly with the proportion of cells in the S phase of the cell cycle. Similarly, Okada et al. (*13*) compared FDG uptake and cellular proliferative activity in 23 patients with malignant lymphoma of the head and neck. They demonstrated that Ki-67 immunoreactivity, which indicates the cells' proliferative activity, as well as the number of cellular mitoses observed under light microscopy increased in proportion to FDG uptake. Duhaylongsod et al. (*14*) reported that glucose metabolism measured by FDG PET correlated with the doubling time of malignant pulmonary lesions, whereas the cellular uptake of

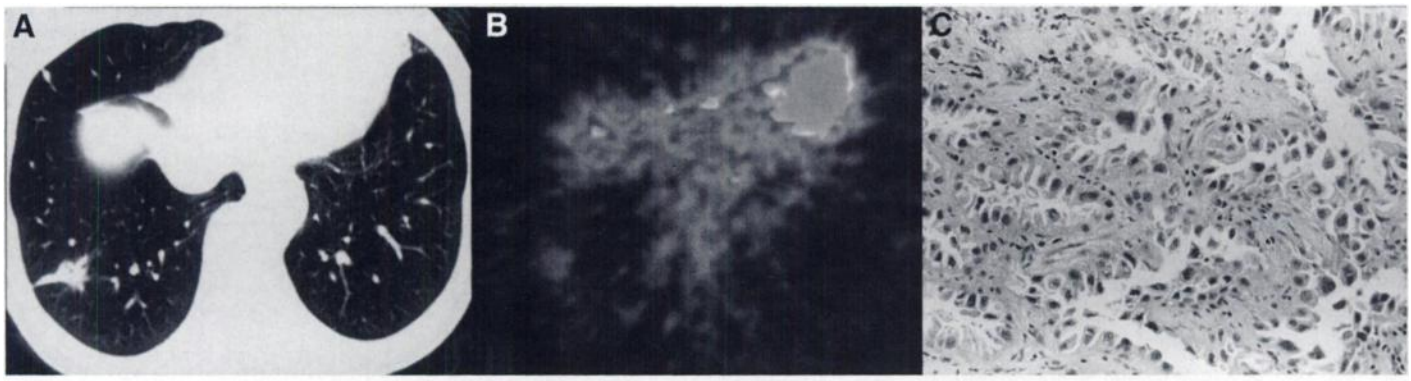

FIGURE 4. Patient 11: well-differentiated adenocarcinoma, 2.0 × 2.0 cm, pT1N0M0. (A) CT image shows a nodule in the right lung. (B) FDG PET shows modest accumulation in the tumor (FDG score 2, SUV 1.24). (C) High-power view shows the growth of an atypical large columnar in the alveolar architecture (hematoxylin and eosin stain; original magnification = × 225).

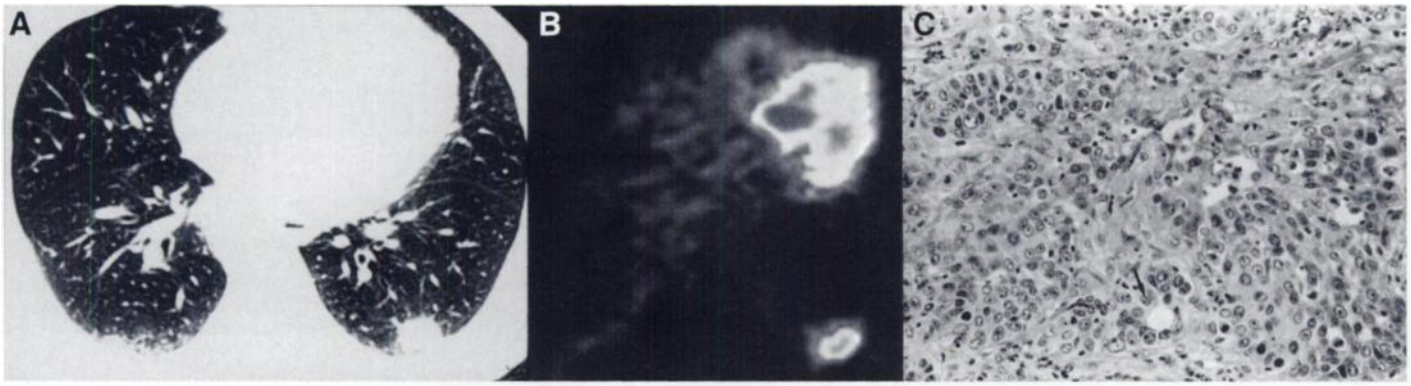

FIGURE 5. Patient 30: poorly differentiated adenocarcinoma, 2.5 × 2.0 cm, pT1N0M0. (A) CT image shows a nodule in the left lung. (B) FDG PET shows hot accumulation in the tumor (FDG score 4, SUV 6.13). (C) High-power view shows the mainly solid growth pattern of anaplastic tumor cells with a focus of tubulus formation (arrow) (hematoxylin and eosin stain; original magnification = × 225).

FDG and the calculated doubling time of indeterminate pulmonary lesions were related inversely. Thus, high levels of glucose metabolism were associated with shorter tumor doubling times, or faster rates of tumor growth. Recently, Higashi et al. (*17*) reported that FDG uptake in nonsmall cell carcinoma of the lung correlated with the percentage of proliferating cell nuclear antigen and Ki-67 positive nuclei. In a microautoradiographic study, Kubota et al. (*28*) reported that viable tumor cells with a fast growth rate had a high FDG uptake. It has been shown that FDG uptake in non-Hodgkin's lymphoma (*29*) and soft-tissue sarcoma (*30*) correlates with malignancy grade. These data suggest that, in certain tumor cell types, glucose metabolism measured by FDG PET varies proportionately with tumor growth or malignancy grade. In our study, BACs' FDG uptake was significantly lower than that of non-BACs, and FDG PET showed negative results on 4 of 7 BACs. As mentioned previously, the mean doubling time for BACs is longer than that for non-BAC adenocarcinomas (*10*). BACs' proliferative potential is lower than that for a well-differentiated adenocarcinoma (*21*). These findings suggest that glucose metabolism measured by FDG PET correlates with proliferative potential of adenocarcinoma of the lung. Thus, FDG PET imaging is biologically true negative for BAC.

Although the number of cases is small, a correlation was seen between FDG uptake and the degree of cell differentiation in adenocarcinoma of the lung. However, among adenocarcinomas sharing the same degree of cell differentiation, FDG uptake has varied somewhat widely. For example, the SUVs of moderately differentiated adenocarcinomas 3.5 cm in size ranged from 2.12–7.06, and the SUVs of some moderately differentiated adenocarcinomas were lower than that of well-differentiated adenocarcinomas. Several reasons may account for this variation in FDG uptake. First, a variety of factors besides the degree of cell differentiation could be related to FDG uptake in adenocarcinoma of the lung. For example, the number of viable cancer cells could be related to FDG uptake. Second, proliferative potential may vary in adenocarcinomas with the same degree of cell differentiation.

A cancer's cell differentiation is one of the parameters for predicting prognosis (*22*) and for selecting treatment regimen for patients with adenocarcinoma of the lung. Unfortunately, the degree of cell differentiation is often difficult to establish by transbronchial lung biopsy or transthoracic needle lung aspiration biopsy. Therefore, the current finding of a correlation between glucose consumption and the degree of cell differentiation is important. A noninvasive diagnostic technique as an aid for establishing the degree of cell differentiation may be of value predicting prognosis and directing treatment regimen selection in patients with lung adenocarcinoma. Additional study is essential to confirm our findings.

CONCLUSION

In this preliminary study, a correlation was seen between glucose metabolism measured by FDG PET and the degree of tumor cell differentiation in adenocarcinoma of the lung. FDG PET may be used as a noninvasive diagnostic technique to aid in establishing the degree of cell differentiation in patients with adenocarcinoma of the lung. FDG PET may show biologically true negative results for bronchioloalveolar carcinoma. This possibility should be kept in mind in the analysis of PET studies of glucose metabolism aimed at differentiating malignant from benign solitary pulmonary nodules.

ACKNOWLEDGMENTS

We thank Nobuo Oya, MD, for his helpful discussion. We also thank the PET technologists and PET chemistry staff of Kanazawa Cardiovascular Hospital for their contributions. This work was supported by a grant for collaborative research (C95–2 for Kotaro Higashi), a grant for project research (P96–2 for Kotaro Higashi and P95–14 for Yoshimichi Ueda) from Kanazawa Medical University and by grants-in aid for scientific research (07671031 for Kotaro Higashi) from the Ministry of Education, Science and Culture, Tokyo, Japan.

REFERENCES

1. Kubota K, Matsuzawa T, Fujiwara T, et al. Differential diagnosis of lung tumor with positron emission tomography: a prospected study. *J Nucl Med* 1990;31:1927–1933.
2. Gupta NC, Frank AR, Dewan NA, et al. Solitary pulmonary nodules: detection of malignancy with PET with 2-[^{18}F]-fluoro-2-deoxy-D-glucose. *Radiology* 1992;184: 441–444.
3. Patz EF, Lowe Vj, Hoffman JM, et al. Focal pulmonary abnormalities: evaluation with ^{18}F-fluorodeoxyglucose PET scanning. *Radiology* 1993;188:487–490.
4. Scott WJ, Schwabe JL, Gupta NC, Dewan NA, Reeb SD, Sugimoto JT. Positron emission tomography of lung tumors and mediastinal lymph nodes using [^{18}F]fluorodeoxyglucose. *Ann Thorac Surg* 1994;58:698–703.
5. Dewan NA, Gupta NC, Redepenning LS, Phalen JJ, Frick NP. Diagnostic efficacy of PET-FDG imaging in solitary pulmonary nodules. *Chest* 1993;104:997–1002.
6. Wahl RL. Positron emission tomography: applications in oncology. In: Murray IPC, Ell PJ, ed. *Nuclear medicine in clinical diagnosis and treatment*, vol. 2. New York: Churchill Livingstone; 1994:801–820.
7. Gupta NC, Maloof J, Gunel E. Probability of malignancy in solitary pulmonary nodules using fluorine-18-FDG and PET. *J Nucl Med* 1996;37:943–948.
8. Jang HJ, Lee KS, Kwon OJ, Rhee CH, Shim YM, Han J. Bronchioloalveolar carcinoma: focal area of ground-glass attenuation at thin-section CT as an early sign. *Radiology* 1996;199:485–488.
9. Clayton F. The spectrum and significance of bronchioloalveolar carcinomas. *Pathl Annu* 1988;23:361–394.
10. Heikkila L, Mattila P, Harjiula A, Sumalainen RJ, Mattila S. Tumor growth rate and its relationship to prognosis in bronchiolo-alveolar and pulmonary adenocarcinoma. *Ann Chir Gynaecol* 1985;74:210–214.
11. Di Chiro G, DeLa Paz RL, Brooks RA, et al. Glucose utilization of cerebral gliomas measured by ^{18}F-fluorodeoxyglucose and positron emission tomography. *Neurology* 1982;32:1323–1329.
12. Minn H, Joensuu H, Ahonen A. Fluorodeoxyglucose imaging: a method to assess the proliferative activity of human cancer in vivo. Comparison with DNA flow cytometry in head and neck tumors. *Cancer* 1988;61:1776–1781.
13. Okada J, Yoshikawa K, Itami M, et al. Positron emission tomography using fluorine-18-fluorodeoxyglucose in malignant lymphoma: a comparison with proliferative activity. *J Nucl Med* 1992;33:325–329.
14. Duhaylongsod FG, Lowe VJ, Patz EF, et al. Lung tumor growth correlations with glucose metabolism measured by fluoride-18-fluorodeoxyglucose positron emission tomography. *Ann Thorac Surg* 1995;60:1348–1362.
15. Rodriguez M, Rehn S, Ahlstom H, Sundstrom C, Glimelius B. Predicting malignancy grade with PET in non-Hodgkin's lymphoma. *J Nucl Med* 1995;36:1790–1796.
16. Nieweg OE, Pruim J, van Ginkel RJ, et al. Fluorine-18-fluorodeoxyglucose PET imaging of soft-tissue sarcoma. *J Nucl Med* 1996;37:257–261.
17. Higashi K, Nishikawa T, Ueda Y, et al. Association of FDG uptake with proliferating cell nuclear antigen, Ki-67 and DNA ploidy pattern in non-small cell lung carcinoma [Abstract]. *J Nucl Med* 1996;37:64.
18. World Health Organization. *Histological typing of lung tumors*, 2nd ed. Geneva: World Health Organization; 1981:25–26.
19. Barsky S, Cameron R, Osann KE, Tomita D, Holmes C. Rising incidence of BAC and its unique clinicopathologic features. *Cancer* 1994;73:1163–1170.
20. Auerbach O, Garfinkel L. The changing pattern of lung carcinoma. *Cancer* 1991;68: 1973–1977.
21. Kitamura H, Kameda Y, Nakamura N, et al. Proliferative potential and p53 overexpression in precursor and early stage lesions of BAC. *Am J pathol* 1995;147:876–887.
22. Noguchi M, Morikawa A, Kawasaki M, et al. Small adenocarcinoma of the lung. *Cancer* 1995;75:2844–2852.
23. Dalquen P, Sauter G, Torhorst J, et al. Nuclear p53 overexpression is an independent prognostic parameter in node-negative non-small cell lung carcinoma. *J Pathol* 1996;178:53–58.
24. Higashi K, Clavo AC, Wahl RL. Does FDG uptake measure proliferative activity of human cancer cells? In vitro comparison with DNA flow cytometry and tritiated thymidine uptake. *J Nucl Med* 1993;34:414–419.
25. Keyes JW. SUV: standard uptake or silly useless value ? *J Nucl Med* 1995;36:1836–1839.
26. Kubota K, Matsuzawa T, Ito M, et al. Lung tumor imaging by positron emission tomography using carbon-11-L-methionine. *J Nucl Med* 1985;26:37- 42.
27. Rusch VW, Reuter VE, Kris MG, et al. Ras oncogene point mutation: an infrequent event in bronchiloalveolar cancer. *J Thorac Cardiovasc Surg* 1992;104:1465–1469.
28. Kubota R, Kubota K, Yamada S, et al. Active and passive mechanisms of ^{18}F-fluorodeoxyglucose uptake by proliferating and prenecrotic cancer cells in vivo: a microautoradiographic study. *J Nucl Med* 1994;35:1067–1075.
29. Radriguez M, Rehn S, Ahlstrom H, Sundstrom C, Glimelius B. Predicting malignancy grade with PET in non-Hodgkin's lymphoma. *J Nucl Med* 1995;36:1790–1796.
30. Nieweg OE, Pruim J, van Ginkel RJ, et al. Fluorine-18-fluorodeoxyglucose PET imaging of soft-tissue sarcoma. *J Nucl Med* 1996;37:257–261.